Isospin diffusion in ^{58}Ni-induced reactions at intermediate energies. II. Dynamical simulations

E. Galichet,[1,2,3,4,*] M. Colonna,[3] B. Borderie,[1] and M. F. Rivet[1]

[1]*Institut de Physique Nucléaire, Université Paris-Sud 11, CNRS/IN2P3, F-91406 Orsay Cedex, France*
[2]*Conservatoire National des Arts et Métiers, F-75141 Paris Cedex 03, France*
[3]*INFN Laboratori Nazionali del Sud, I-95123 Catania, Italy*
[4]*INFN Sez. di Catania and Dipartimento di Fisica, Università di Catania, Italy*

We study isospin effects in semiperipheral collisions above the Fermi energy by considering the symmetric ^{58}Ni + ^{58}Ni and the asymmetric ^{58}Ni + ^{197}Au reactions over the incident energy range 52A–74A MeV. A microscopic transport model with two different parametrizations of the symmetry energy term is used to investigate the isotopic content of pre-equilibrium emission and the N/Z diffusion process. Simulations are also compared to experimental data obtained with the INDRA array and provide information on the degree of isospin equilibration observed in Ni + Au collisions. A better overall agreement between data and simulations is obtained when using a symmetry term that linearly increases with nuclear density.

PACS number(s): 25.70.−z, 24.10.−i

I. INTRODUCTION

Collisions between nuclei with different charge asymmetries may carry important information on the structure of the nuclear equation of state (EOS) symmetry term in density and temperature regions away from the normal value, which may be encountered along the reaction path [1,2]. For instance, the symmetry energy behavior influences reaction processes, such as fragmentation, pre-equilibrium emission, and N/Z equilibration between the two collisional partners [3–11]. Among the sensitive observables, in semiperipheral collisions, one can look at the isotopic content of light particle and intermediate mass fragment (IMF) emission and at the asymmetry (N/Z) of the reconstructed quasi-projectiles (QP) and quasi-targets (QT) [7,8,12]. The degree of equilibration, which is related to the interplay between the reaction time and the typical time for isospin transport, can give information about important transport properties, such as drift and diffusion coefficients, and their relation with the density dependence of the symmetry energy.

In this article we undertake this kind of investigation by studying isospin transport effects on the reaction dynamics in collisions with impact parameters between 4 and 12 fm. Two systems, with the same projectile, ^{58}Ni, and two different targets (^{58}Ni and ^{197}Au), are considered at incident energies of 52A and 74A MeV. The N/Z ratio of the two composite systems is $N/Z = 1.07$ for Ni + Ni and $N/Z = 1.38$ for Ni + Au. The choice of the two systems and beam energies will allow us to study isospin effects under different conditions of charge (and mass) asymmetry and how they evolve as a function of the energy deposited into the system. In the symmetric Ni + Ni system isospin effects are essentially due to the pre-equilibrium emission. However, in the charge (and mass) asymmetric reactions, one can observe isospin transport between the two partners. The dependence of these mechanisms on the symmetry energy behavior is discussed.

The article is organized as follows. In Sec. II, we describe the model used and we present the results obtained and then, in Sec. III, we discuss the role of the isospin degree of freedom on the reaction dynamics and the comparison with some experimental data. Conclusions are drawn in Sec. IV.

II. RESULTS OF BNV CODE

A. Evolution in phase space

We follow the reaction dynamics solving the BNV transport equation, which describes the evolution of the one-body distribution function according to the nuclear mean field and including the effects of two-body collisions [13]. The test particle prescription is adopted, using the TWINGO code [14] with 50 test particles per nucleon. The main ingredients that enter this equation are the nuclear matter compressibility, the symmetry energy term and its density dependence, and the nucleon-nucleon cross section. We take a soft isoscalar equation of state, with a compressibility modulus $K = 200$ MeV, which is favored, e.g., from flow studies or from the confrontation data-dynamical simulations at intermediate energies [15,16]. Two different prescriptions for the behavior of the symmetry energy are used to study the sensitivity of the results to the considered parametrization: an "asy-stiff" case for which the potential symmetry term linearly increases with nuclear density [$E_{sym}(\rho) = E_{sym}(\rho_0)(\rho/\rho_0)$], where ρ_0 is the nuclear saturation density, and an "asy-soft" case using the SKM* parametrization, which exhibits a $(\rho/\rho_0)^{0.6}$ dependence (see Ref. [5] for more details). The free nucleon-nucleon cross section with its angular, energy, and isospin dependence was used. For the two reactions, we ran different impact parameters, from $b = 4$ fm to $b = 10$ fm for the Ni + Ni system and from $b = 4$ fm to $b = 12$ fm for the Ni + Au system. For each impact parameter 10 events were produced (one event represents already the mean trajectory of the reaction) for the two cases of symmetry energy

_____
*Corresponding author: galichet@ipno.in2p3.fr

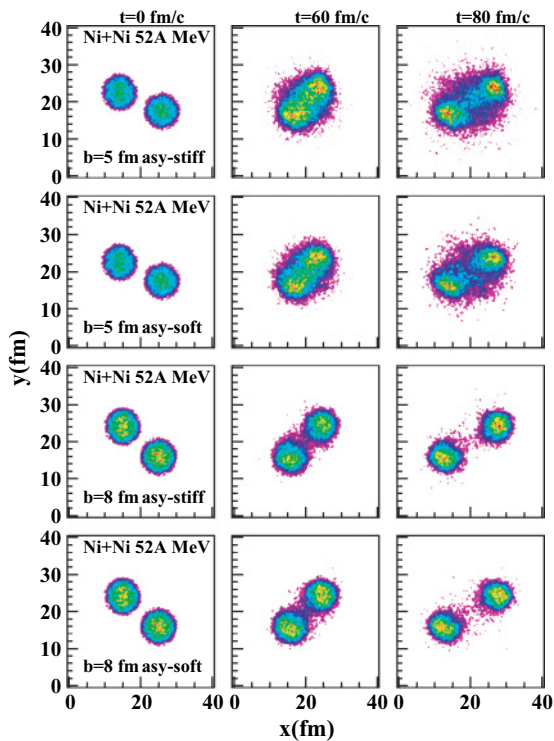FIG. 1. (Color online) Density plots for Ni + Ni collisions at 52A MeV.

FIG. 2. (Color online) Density plots for Ni + Au collisions at 52A MeV.

parametrization. In the following, except for Figs. 1 and 2, the results shown are averaged over the 10 events for each impact parameter. This reduces the fluctuations due to the use of a finite number of test particles in the simulations. In Figs. 1 and 2 the time evolution of density contours in the reaction plane is displayed for two impact parameters and the two parametrizations of the symmetry energy term, asy-soft and asy-stiff.

In general the asy-stiff EOS can be linked to a more repulsive dynamics. Indeed, in this case, the system feels a stronger repulsion in the first stage of the collisions, due to the increased value of the symmetry energy above normal density. However, in proton-rich systems, the larger value of E_{sym} can lead also to a larger pre-equilibrium proton emission. Hence, finally, because of the lowering of Coulomb repulsion among the reaction partners, they can interact for a longer time, favoring the occurrence of dissipative mechanisms [17].

Indeed, in the 52A MeV Ni + Ni case, at $t = 80$ fm/c ($b = 5$ fm), a more dissipative neck dynamics is observed in the asy-stiff case. At $b = 8$ fm the reaction shows essentially a binary character for both EOS. Similar effects are observed for the Ni + Ni reaction at 74A MeV. In this Ni + Au case, we face a different situation, because now the system is neutron rich, apart from the fact that it is also asymmetric in mass and has a larger size. For neutron-rich colliding ions the asy-soft choice leads to a little more dissipative dynamics. We can see in Fig. 2 that, at $b = 5$ fm, the reaction appears quite dissipative and it is difficult to distinguish the projectile from the target, especially in the soft case. At $b = 10$ fm, the collision is essentially binary. One can see some particles in between projectile and target regions,
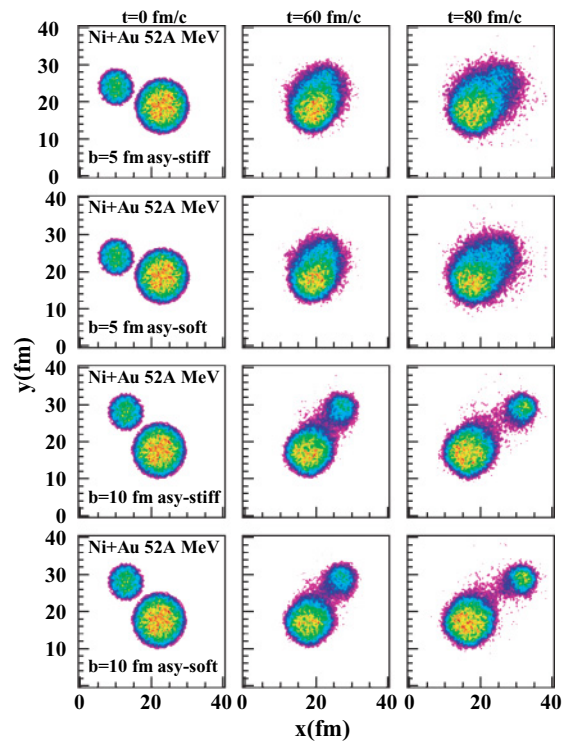
mostly due to pre-equilibrium emission, and the two EOS give very similar results. However, in general the difference on the reaction path between the asy-soft and asy-stiff choice appears quite small and one must explore the behavior of other observables more sensitive to the symmetry energy.

B. Observables

1. Mass and excitation energy of primary QP/QT

We have simulated the reactions until $t = 200$ fm/c. The properties of the two main partners of the collision are considered at the time when they reseparate after interaction. We call this time t_{sep}. At t_{sep}, which differs for each impact parameter, QP and QT are well defined. A clusterization procedure (in $\vec{r}$ space) was used to separate the different products of the reaction [18]. Because of the mean-field approximation, only heavy fragments and IMFs can be reconstructed with this procedure in a reliable way, whereas the yield of complex particles is underestimated and the number of free nucleons overestimated. Thus we can obtain the mass, charge, and excitation energy of the two main partners and all possible fragments. The mass and the excitation energy of QT and QP are represented in Fig. 3 for the two systems, the two energies, and the two choices of symmetry energy term, as a function of the impact parameter.

The mass of QT and QP decreases when going toward more central collisions. This is due first to pre-equilibrium particle emission. Moreover, in some cases, an IMF can originate from the overlap region. For the Ni + Ni system the mass of both QP and QT is little sensitive to the choice of the interaction.
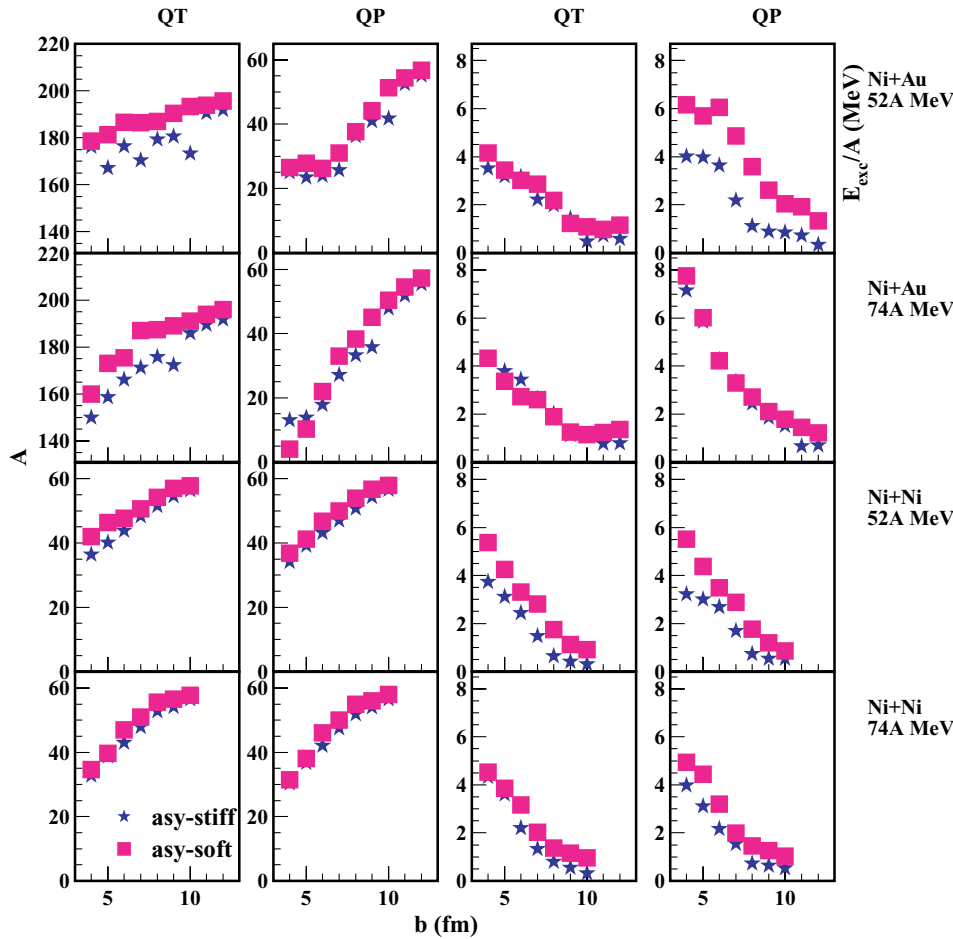
FIG. 3. (Color online) Masses (columns 1 and 2, left) and excitation energy per nucleon (columns 3 and 4, right) of the quasi-target (QT) and the quasi-projectile (QP) as a function of the impact parameter, for the two reactions and the two energies. The stars correspond to the asy-stiff case and the squares to the asy-soft case.

On the contrary for the Ni + Au system the two equations give different results for the QT. For both incident energies the mass in the asy-soft case is higher than that in the asy-stiff case. Indeed with the asy-stiff equation the production of an IMF between the two partners is more probable, with respect to the re-absorption of the neck region. This IMF comes essentially from the target; thus its emission does not affect the mass of the QP, whose mass is then independent of the chosen equation of state. This explains the oscillatory behavior of the QT mass in the asy-stiff case for the Ni + Au system at 52A MeV.

The excitation energy per nucleon of QT and QP becomes higher for central collisions in all cases. For the symmetric Ni + Ni system, the energies of the two partners are equal, as expected. They do not depend on the EOS at 74A MeV, and they are higher with the asy-soft EOS at 52A MeV, due to the less energetic pre-equilibrium emission in this case. In the Ni + Au system, at 52A MeV, the excitation energies of the QP strongly depend on the EOS, indicating that more dissipation occurs in the asy-soft case. The effect is less evident on the QT side, as expected, because the percentage of nucleons involved in dissipative mechanisms (in these semiperipheral collisions) is smaller for the system with the largest mass. It is interesting to notice also that, at 74A MeV, the QT keeps almost the same value of excitation energy as the one obtained at 52A MeV, whereas only for the QP is an increase of excitation energy observed for the most central

collisions. At 74A MeV the two asy-EOS lead to very similar results.

Globally, at the highest incident energy and for both systems, probably because of the shorter interaction times, no influence of the EOS appears on the excitation energies. Conversely the symmetry term does act on the excitation energies at 52A MeV.

2. N/Z ratio of the quasi-projectile

Let us turn to isospin-dependent observables, such as the N/Z ratio of the quasi-projectile. The isospin ratio of the projectile, ^{58}Ni, and of the composite Ni + Ni system is 1.07 while isospin ratios of the Au target and of the Ni + Au system are, respectively, 1.49 and 1.38. After collision the isospin content of the QP is expected to depend on the target, remaining unchanged for the symmetric system, and lying somewhere between those of the projectile and of the composite system, depending on the interaction and the isospin equilibration times for the Ni + Au system. In Fig. 4 we show the N/Z of the quasi-projectile, as obtained by averaging the results of the 10 BNV events. The associated errors are of the order of 0.015. The N/Z ratio increases with the centrality of the collision for the two systems and the two energies.
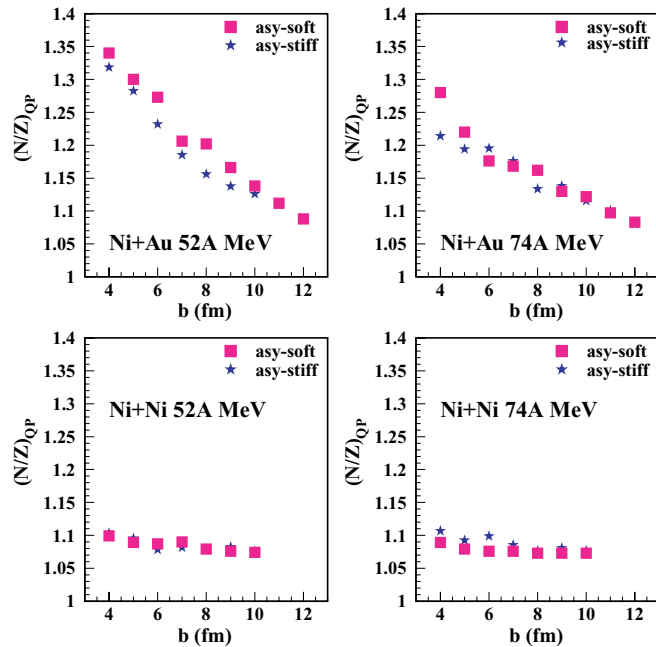
FIG. 4. (Color online) Isospin ratio of the quasi-projectile as a function of the impact parameter, for the two reactions and the two energies. The stars correspond to the asy-stiff case and the squares to the asy-soft case.

FIG. 5. (Color online) Correlation between $E_{\rm diss}/E_{\rm c.m.}$ and the impact parameter for the two reactions and the two energies. The stars correspond to the asy-stiff case and the squares to the asy-soft case.

For the Ni + Ni system the variation of N/Z with centrality is small and attributed to pre-equilibrium emission. Little dependence on the EOS appears at 52A MeV, while N/Z grows slightly higher at 74A MeV for the stiff case. Indeed, with a stiff EOS, more protons are emitted during the pre-equilibrium stage. This effect increases with the incident energy. On the contrary, the asy-soft case tends to emit more pre-equilibrium neutrons leading to a lower N/Z ratio [19].

The evolution with centrality is much more pronounced for the neutron-rich and asymmetric Ni + Au system. In addition to pre-equilibrium effects, isospin transport takes place between the two partners of the collision, which increases with the violence of the collision. N/Z is mostly higher in the asy-soft than in the asy-stiff case (which is less dissipative, as seen above) for the two energies. Thus the N/Z diffusion appears related to the degree of dissipation reached in the system and to the driving force provided by the symmetry term of the nuclear EOS, which speeds up the isospin equilibration among the reaction partners [2,7,9]. The largest value reached, at $b = 4$ fm, is lower at 74A MeV than at 52A MeV; this may be attributed to the shorter reaction times and to the fact that the collision becomes more transparent. It must be underlined that isospin equilibration is nearly reached at the lower energy for the soft EOS, at $b = 4$ fm. An asy-soft EOS thus favors isospin equilibration between the two partners, as found also in other recent theoretical investigations [6,7,9,20].

In conclusion we can say that the effect of the EOS on the quasi-projectile N/Z content appears essentially in two ways: in an asymmetric system (Ni + Au case) the effect will be seen mostly on the isospin equilibration between the two partners
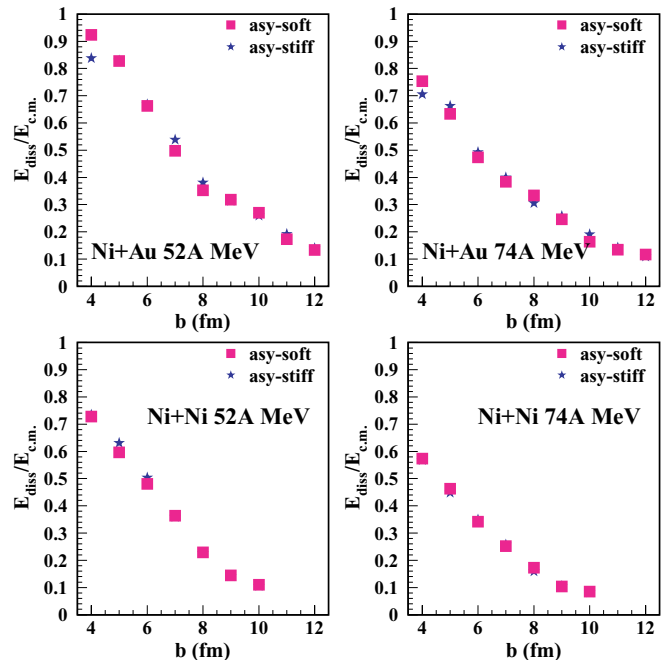
of the collision, whereas for a symmetric system the effect will react essentially on the pre-equilibrium emission.

III. COMPARISON WITH EXPERIMENTAL DATA

A. Excitation energy

To compare results of the present model with experimental data collected with the INDRA detector, the same sorting must be adopted [12]. The chosen sorting variable is the energy dissipation calculated, as in the experimental analysis, from the relative velocity between QP and QT [12]. The correlation between the calculated dissipated energy normalized to the center of mass energy—called $E_{\rm diss}/E_{\rm c.m.}$ in the following—and the impact parameter is displayed in Fig. 5. In all cases the two quantities are strongly correlated, which confirms that $E_{\rm diss}$ is a good measure of the centrality of the collision. It should be stressed that a given relative dissipation $E_{\rm diss}/E_{\rm c.m.}$ corresponds for the different reactions to different impact parameters. The correlation does not depend much on the employed equation of state, although for the Ni + Au system a tendency toward more dissipation in the asy-soft case starts to be visible below $b = 5$ fm. So, this sorting variable does not reflect exactly the dissipation energy deposited into the system, which, as seen in Fig. 5, does depend on the asy-EOS, especially for the 52A MeV reactions. This is because in the evaluation of $E_{\rm diss}$ the effects of pre-equilibrium emission are neglected.

With the help of the dissipated energy $E_{\rm diss}$ as a sorting variable, the behavior of some observables can be followed
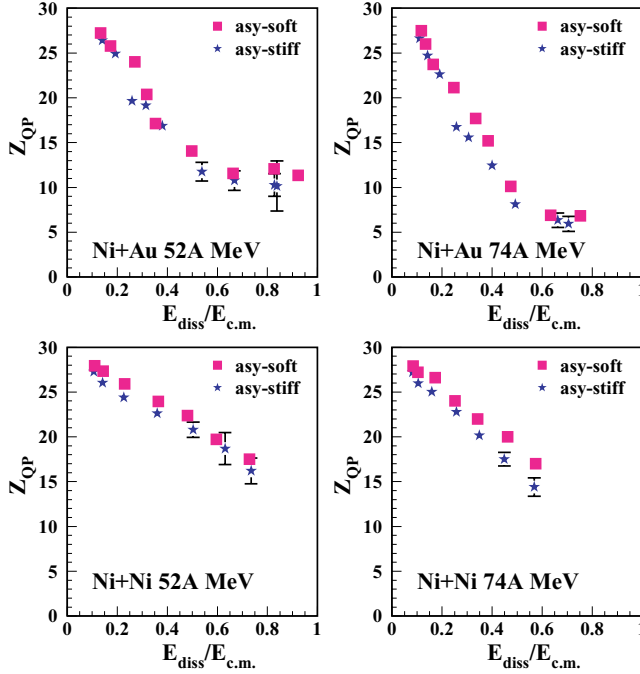
FIG. 6. (Color online) Calculated charge of the primary quasi-projectile vs $E_{\text{diss}}/E_{\text{c.m.}}$, for the two reactions and the two energies. The stars correspond to the asy-stiff case and the squares to the asy-soft case. Statistical error bars are shown.

FIG. 7. (Color online) Charge of the quasi-projectile residue vs $E_{\text{diss}}/E_{\text{c.m.}}$, for the two reactions and the two energies. The squares correspond to the asy-soft case + SIMON, the stars to the asy-stiff case + SIMON, and the circles to the experimental data.

versus the violence of the collision. For comparisons between calculated and experimental data the hot primary quasi-projectiles were cooled down with the proper part of the SIMON code [21].

B. Charge of the quasi-projectile

Figure 6 shows the calculated charge of primary QP (defined at t_{sep}) as a function of dissipation. Fragments coming from the neck region were not considered in the evaluation of Z_{QP}; it was, however, checked that taking them into account changes very slightly the QP charge values. The variation remains within the statistical errors, which are represented only in the asy-stiff case in Fig. 6 for better visibility. These errors only exceed the size of the symbols for the more dissipative collisions.

As expected, Z_{QP} decreases with the increase of E_{diss} for the two systems and the two energies. For the Ni + Au system the charge decreases down to $Z \approx 10$ at 52A MeV and to $Z \approx 5$ at 74A MeV, because of a larger pre-equilibrium emission (see Sec. II B1). For the Ni + Ni system the charge remains higher ($Z \approx 17$ and $Z \approx 15$ for 52A and 74A MeV, respectively), even at similar percentages of dissipation of the available energy. The two equations of state give rather similar behaviors. However, the soft equation of state gives results that are systematically above the ones obtained in the stiff case. The comparison of the charge of the final QP residue, obtained with the two asy-parameterizations, with the experimental values is shown in Fig. 7. For experimental data, averages and standard deviations of the distribution of the heaviest fragment
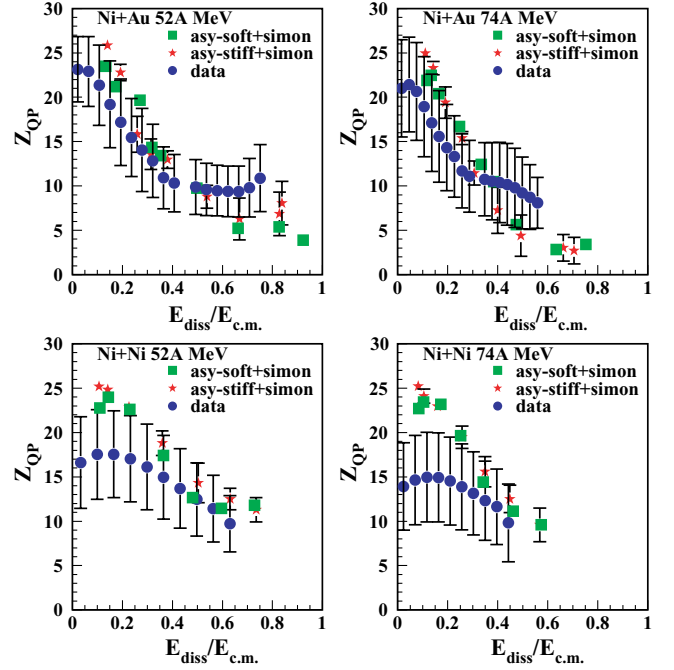
measured by INDRA [12] are displayed. Because of geometry and trigger effects (see Ref. [12]) the more peripheral collisions were rejected for the Ni + Ni system, leading to an apparent decrease of the charge of the detected QP for the lower values of the excitation energy. At higher dissipation, for the two systems, data well follow the theoretical trend and charges of final QP are within the standard deviation of the data. In all cases one can stress that the agreement between calculation and experiment is better for the more central collisions.

C. N/Z ratio as a function of the dissipation

The N/Z ratio of primary QP as a function of E_{diss} is reported in Fig. 8. The lines represent the results of a linear fit. These results, plotted versus b, are discussed in Sec. II B2; the observed trends are not modified when the dissipation is used as a scale for the violence of the collision (see also Sec. III A). Particularly, N/Z equilibration is nearly reached in the Ni + Au system at 52A MeV, with an asy-soft EOS, when about 80% of the available energy has been dissipated. In the same figure also plotted are the results concerning the de-excitation step, with the variable called $(N/Z)_{\text{CP}}$ defined for experimental data. Isotopes included in the calculation of the variable are those evaporated by the hot QP. The values of $(N/Z)_{\text{CP}}$ are always smaller than the N/Z of the primary QP. At low dissipation, in all cases, the value starts at 1 instead of 1.07, due to the dominance of α particles. The evolution of $(N/Z)_{\text{CP}}$ with $E_{\text{diss}}/E_{\text{c.m.}}$ is generally flatter than the $(N/Z)_{\text{QP}}$; however, the differences between the results of the two parametrizations are more pronounced for $(N/Z)_{\text{CP}}$, with
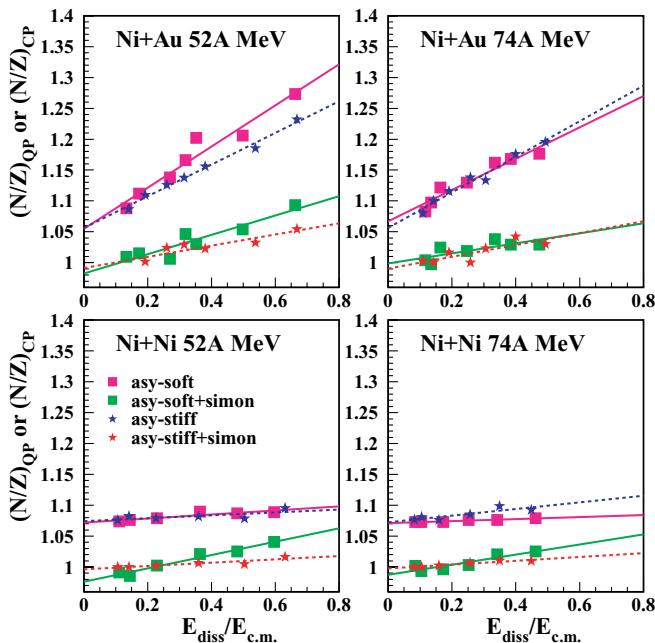
FIG. 8. (Color online) Isospin ratio of the quasi-projectile vs $E_{\text{diss}}/E_{\text{c.m.}}$, for the two reactions and the two energies. For the asy-stiff calculation, black stars and dotted lines represent the $(N/Z)_{\text{QP}}$ and grey stars and dotted lines represent the $(N/Z)_{\text{CP}}$ (BNV calculation followed by SIMON). The same conventions for the asy-soft case are displayed by squares and solid lines. The lines correspond to linear fits.

FIG. 9. (Color online) Isospin ratio of complex particles for Ni quasi-projectile vs $E_{\text{diss}}/E_{\text{c.m.}}$, for the two reactions and the two energies. Circles correspond to the experimental data: open for data forward of the N-N velocity [12], solid for data forward in the QP frame. Experimental error bars are within the size of the symbols. Dotted lines and solid lines are as in Fig. 8 and hatched zones correspond to error bars from simulations.

respect to $(N/Z)_{\text{QP}}$, especially at $52A$ MeV. This is because excitation energies are larger in the asy-soft case and this favors the emission of neutron-richer particles, thus enhancing the effect due to the larger N/Z value observed in the asy-soft case for the QP. Only for the reaction Ni + Ni at $74A$ MeV, where the N/Z of the QP is higher in the asy-stiff case, do the effects due to the de-excitation modify the initial trend imposed by the dynamical evolution. For the Ni + Au case at $52A$ MeV, for instance, the slopes associated with the evolution of $(N/Z)_{\text{QP}}$ and $(N/Z)_{\text{CP}}$ with $E_{\text{diss}}/E_{\text{c.m.}}$, obtained with the two parametrizations, differ by 20 and 40%, respectively. $(N/Z)_{\text{CP}}$ is thus a good indicator of isospin transport effects and is sensitive to the asy-EOS, though no direct conclusion concerning the reach of isospin equilibration among the two reaction partners can be derived from this variable. It should be noticed that the difference observed for $(N/Z)_{\text{QP}}$, between the two parametrizations, is in agreement with recent calculations performed on other systems in the same energy range [20].

A comparison of calculated and experimental values of $(N/Z)_{\text{CP}}$ is shown in Fig. 9. The results presented in the accompanying article [12] correspond to open circles; they are above the calculated $(N/Z)_{\text{CP}}$ at low dissipation but values get closer at high dissipation. We remind that these experimental values correspond to forward emitted particles in the nucleon-nucleon frame, because of the difficulty to define a QP source. For comparison with the values calculated with BNV + SIMON, we need a variable more representative of the QP de-excitation properties. Toward this goal a second
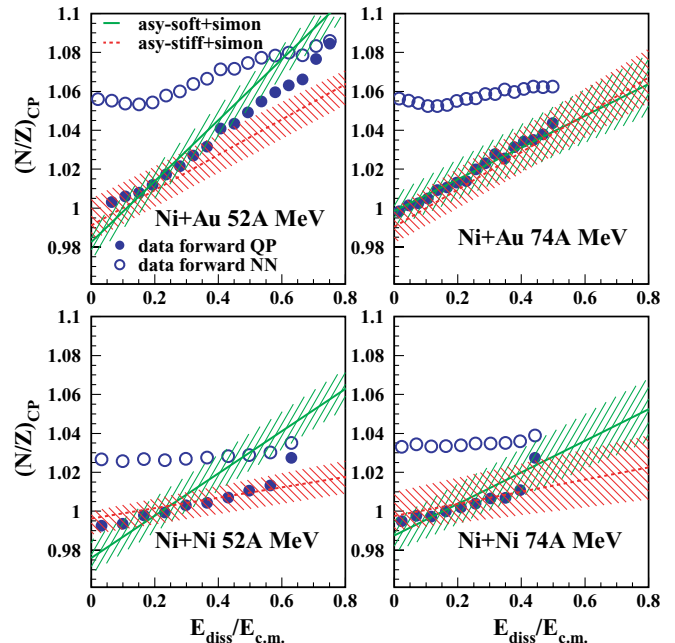
experimental value of $(N/Z)_{\text{CP}}$ was built with forward emitted particles in the QP frame. The values are remarkably close to the BNV + SIMON data, for all systems, particularly for the asy-stiff case. They are lower than those built with forward emitted particles in the N-N frame at low dissipation, which indicates that indeed midrapidity emission is more neutron-rich for the complex particles considered in the variable $(N/Z)_{\text{CP}}$. Both experimental values (forward N-N and forward QP) present the same trend, namely, no or very little evolution with dissipation for Ni + Ni and an increase with the violence of the collision for Ni + Au. For Ni + Au at $52A$ MeV, they become equal at high dissipation. This gives a strong experimental indication that N/Z equilibration has been reached.

D. Summary of the main findings

Following the comparison between calculations with two EOS and between calculations and experimental data, several important points can be stressed.

(i) BNV calculations show a very good correlation between the impact parameter and the variable E_{diss} calculated as in experiment: E_{diss} appears as a good indicator of the violence of the collision.

(ii) The differences between the two EOS are small, which reflects the fact that in the studied collisions nuclear densities keep values close to the normal one.

(iii) The secondary decay effect is very important and, in almost all cases, it reduces the sensitivity of the proposed isospin observable $(N/Z)_{\rm CP}$ with $E_{\rm diss}/E_{\rm c.m.}$.

(iv) Calculations support the experimental observation of the significant increase of the (N/Z) observable for QP in the Ni + Au reactions as a function of the centrality of the collisions. This appears related to isospin equilibration between the two reaction partners.

(v) The value of $(N/Z)_{\rm CP}$ calculated with BNV + SIMON well matches the experimental data obtained from the forward emitted products in the QP frame for the whole dissipation range studied. This indicates that the products emitted forward in the QP frame are well representative of the QP de-excitation properties.

(vi) Globally the asy-stiff case better matches the experimental data for both systems. In particular, the behavior of $(N/Z)_{\rm CP}$ with respect to $E_{\rm diss}/E_{\rm c.m.}$ is better reproduced by the asy-stiff interaction. A similar interaction with free nucleon-nucleon cross section was also used in a BUU transport code to well reproduce isospin diffusion deduced from an isoscaling analysis for ^{124}Sn + ^{112}Sn at 50A MeV [9].

(vii) BNV calculations show that isospin equilibration is quasi-reached at the higher dissipation (impact parameter around 5 fm) for the Ni + Au system at 52A MeV. The same conclusion can be directly deduced experimentally from the observation that the $(N/Z)_{\rm CP}$ forward of the N-N velocity and forward in the QP frame become equal.

(viii) Finally, the isospin equilibration time for reactions in the Fermi energy domain, as considered here, can be estimated at 130 ± 10 fm/c; this time is the time interval when the dinuclear system remains in interaction, for the most dissipative binary collisions studied at 52A MeV.

IV. CONCLUSION

In this article we have studied isospin effects in semiperipheral nuclear collisions above the Fermi energy, with different conditions of mass and charge asymmetry, using different equations of state: asy-soft and asy-stiff. Toward this end, we have compared results obtained on quasi-projectiles, in two different reactions with the same projectile: ^{58}Ni + ^{58}Ni and ^{58}Ni + ^{197}Au, at incident energies of 52A and 74A MeV. The present analysis is an alternative to both the isoscaling analysis obtained from an average experimental impact parameter [7,9] and the pre-equilibrium neutron-to-proton ratios that correspond to events distributed over an impact parameter range [11,22,23]. Here we study isospin transfer as a function of dissipation or centrality in collisions for two beam energies, looking directly at the average isotopic content of the emitted light particles. Simulations show that for the Ni + Ni system, the N/Z of the quasi-projectile is essentially determined by proton-rich pre-equilibrium emission, and so the N/Z slightly increases with centrality. The effect is more pronounced using an asy-stiff equation of state. For the Ni + Au system isospin transport takes place and the N/Z is larger in the asy-soft case. Excitation energies are also larger in the asy-soft case, increasing the N/Z of the emitted particles. Hence in the Ni + Ni case we observe a kind of compensation between the trend imposed by the dynamical evolution and the secondary decay, whereas in the Ni + Au case the two effects act in the same direction. Finally we find a better overall agreement with experimental data for the asy-stiff case corresponding to a symmetry term linearly increasing with nuclear density. Moreover more precise information concerning the isospin equilibration time, as compared to the conclusions of the experimental joint article, is obtained. At 52A MeV for the Ni + Au and the most dissipative collisions we can infer from the data-model comparison that isospin equilibration is reached at 130 ± 10 fm/c. Another very interesting result comes from the present study: as far as the N/Z content is concerned, the chemical composition of the quasi-projectile forward emission appears tobe a very good representation of the composition of the entire quasi-projectile source. Such an observation seems to validate a posteriori this kind of selection frequently used to characterize the QP de-excitation properties.

[1] *Isospin Physics in Heavy-Ion Collisions at Intermediate Energies*, edited by Bao-An Li and W. U. Schröder (NOVA Science, New York, 2001).

[2] V. Baran, M. Colonna, V. Greco, and M. Di Toro, Phys. Rep. **410**, 335 (2005).

[3] H. Xu *et al.*, Phys. Rev. Lett. **85**, 716 (2000).

[4] Bao-An Li, C. M. Ko, and Zhongzhou Ren, Phys. Rev. Lett. **78**, 1644 (1997).

[5] V. Baran *et al.*, Nucl. Phys. **A703**, 603 (2002).

[6] L. Shi and P. Danielewicz, Phys. Rev. C **68**, 064604 (2003).

[7] M. B. Tsang *et al.*, Phys. Rev. Lett. **92**, 062701 (2004).

[8] D. V. Shetty *et al.*, Phys. Rev. C **70**, 011601(R) (2004).

[9] L.-W. Chen, C. M. Ko, and B.-A. Li, Phys. Rev. Lett. **94**, 032701 (2005).

[10] J. Rizzo, M. Colonna, and M. Di Toro, Phys. Rev. C **72**, 064609 (2005).

[11] M. A. Famiano *et al.*, Phys. Rev. Lett. **97**, 052701 (2006).

[12] E. Galichet *et al.*, Phys. Rev. C **79**, 064614 (2009).

[13] E. A. Uehling and G. E. Uhlenbeck, Phys. Rev. **43**, 552 (1933); A. Bonasera, F. Gulminelli, and J. Molitoris, Phys. Rep. **243**, 1 (1994).

[14] A. Guarnera, M. Colonna, and Ph. Chomaz, Phys. Lett. **B373**, 267 (1996).

[15] P. Danielewicz, R. Lacey, and W. G. Lynch, Science **298**, 1592 (2002).

[16] B. Borderie and M. F. Rivet, Prog. Part. Nucl. Phys. **61**, 551 (2008).

[17] M. Colonna, M. Di Toro, G. Fabbri, and S. Maccarone, Phys. Rev. C **57**, 1410 (1998).

[18] A. Bonasera, M. Colonna, M. Di Toro *et al.*, Phys. Lett. **B244**, 169 (1990).

[19] R. Lionti, V. Baran, M. Colonna, and M. Di Toro, Phys. Lett. **B625**, 33 (2005).

[20] V. Baran, M. Colonna, M. Di Toro, M. Zielinska-Pfabe, and H. H. Wolter, Phys. Rev. C **72**, 064620 (2005); J. Rizzo, M. Colonna, V. Baran *et al.*, Nucl. Phys. **A806**, 79 (2008).

[21] D. Durand, Nucl. Phys. **A541**, 266 (1992).

[22] Bao-An Li *et al.*, Phys. Lett. **B634**, 378 (2006).

[23] Yingxun Zhang *et al.*, Phys. Lett. **B664**, 145 (2008).